Characterizing the epidemiological interactions between influenza and respiratory syncytial viruses and their implications for epidemic control

Sarah C. Kramer[1], Jean-Sébastien Casalegno[2,3,4], Matthieu Domenech de Cellès[1,*]

1. Max Planck Institute for Infection Biology, Infectious Disease Epidemiology group, Charitéplatz 1, Campus Charité Mitte, 10117 Berlin, Germany
2. Hospices Civils de Lyon, Hôpital de la Croix-Rousse, Centre de Biologie Nord, Institut des Agents Infectieux, Laboratoire de Virologie, Lyon, France
3. Centre national de référence des virus des infections respiratoires (dont la grippe), Hôpital de la Croix-Rousse, Lyon, France
4. Centre International de Recherche en Infectiologie (CIRI), Laboratoire de Virologie et Pathologie Humaine - VirPath Team, INSERM U1111, CNRS UMR5308, École Normale Supérieure de Lyon, Lyon, France

* Corresponding author: Dr. Matthieu Domenech de Cellès, Max Planck Institute for Infection Biology, Charitéplatz 1, Campus Charité Mitte, 10117 Berlin, Germany

Keywords: Influenza viruses; Respiratory Syncytial Viruses; Viral Interference; Mathematical Models; Public Health

Abstract

Pathogen-pathogen interactions represent a critical but little-understood feature of infectious disease dynamics. In particular, experimental evidence suggests that influenza viruses and respiratory syncytial viruses (RSV) compete with each other, such that infection with one confers temporary protection against the other. However, such interactions are challenging to study using common epidemiologic methods. Here, we use a mathematical modeling approach, in conjunction with detailed surveillance data from Hong Kong, to infer the strength and duration of the interaction between influenza and RSV. We further utilize our model to evaluate the potential of live attenuated influenza vaccines (LAIV) as a novel strategy to control RSV epidemics. We find evidence of strong, bidirectional interference, such that infection with either virus yields almost complete protection against infection with the other for two to four months. Furthermore, we demonstrate that the likely impact of widespread LAIV use depends on underlying viral circulation patterns. More broadly, we highlight the utility of mathematical models as a tool to characterize interactions and predict the indirect effects of vaccines.

Introduction

Although pathogens are often studied in isolation, mounting evidence suggests that interactions, in which one pathogen impacts the risk of infection or disease due to another pathogen, are a common and important feature governing their epidemiological dynamics[1–3]. These interactions can be characterized according to their major components: they may be positive (i.e., infection with one pathogen facilitates or exacerbates infection with another) or negative (i.e., infection with one pathogen inhibits or mitigates infection with another); may have a strong or a weak effect; may be short-lived or long-lasting; may be symmetric (i.e., both pathogens impact each other in the same way) or asymmetric; and may operate according to a range of biological mechanisms, including changes to the immune response or to host cell gene expression[4].

Although the mechanisms underlying these interactions often occur at the individual level, the existence of an interaction can lead to significant, and sometimes unexpected, consequences at the population level[5,6]. For example, if infection with one pathogen increases susceptibility to another, as demonstrated for influenza viruses and the *Streptococcus pneumoniae* bacterium[7,8], public health measures designed to reduce infection with the first pathogen may also succeed in combating the cocirculating pathogen. Conversely, if infection with one pathogen reduces susceptibility to another, then measures to control this pathogen may lead to unintentional increases in the burden of the other. For example, seasonal influenza vaccination has been associated with an increased risk of both pandemic influenza H1N1 2009 (H1N1pdm09)[9] and non-influenza infection[10], a finding that could be due to the existence of negative interactions. For this reason, it is critical that interactions between pathogens be understood and taken into account when developing public health policy.

One such interaction of public health relevance may exist between influenza and respiratory syncytial viruses (RSV). Both influenza and RSV represent significant public health

threats, particularly in young children and the elderly[11]. Existing research suggests that there may be a strong, negative interaction between these two viruses. For example, experimental studies have found that ferrets and mice infected with influenza were less likely to be infected with RSV upon challenge[12,13] and that infection with either of the two viruses can reduce morbidity upon subsequent infection with the other[12,14,15]. In human populations, this interaction is tentatively supported by epidemiologic observations revealing delays in RSV epidemics occurring during and immediately after the 2009 influenza pandemic[16,17]. This suggests a potential novel control measure for RSV: if vaccination with a live attenuated influenza vaccine (LAIV) induces an immune response similar to natural infection, such vaccines could be used to reduce RSV burden[18]. This is a particularly important strategy to explore, given that, despite promising candidates, no licensed vaccines against RSV are currently available[19].

However, existing epidemiologic evidence is insufficient to confirm the existence of this interaction: seemingly intuitive study designs, which focus on observable metrics such as phase differences and the prevalence of coinfections, are prone to mischaracterizing both the strength and direction of interactions[6,20] and the applicability of studies in animal models to human populations is unclear. Furthermore, interactions are challenging to study due to the large number of components needed to fully characterize them[4]. Mathematical modeling approaches offer a promising alternative to standard epidemiologic study designs because they can capture the complex and nonlinear dynamics inherent to infectious disease transmission and explicitly account for the mechanisms underlying an interaction[5,20,22]. Mathematical models are also an essential tool for exploring the impacts of prospective public health control measures, as they can be used to generate counterfactual scenarios[5]. Despite this potential, to our knowledge, only one modeling study has attempted to infer the characteristics of the

interaction between influenza and RSV and found inconclusive results regarding the strength and duration of cross-protection[23].

Here, we fit a mathematical model of influenza and RSV cocirculation to multiple seasons of data from Hong Kong to infer the strength and duration of the interaction between RSV and different (sub)types of influenza at the individual level. Additionally, we use our model to assess the potential impact of widespread LAIV use on the burden of RSV. We find that infection with influenza or RSV strongly reduces susceptibility to the other virus and that this reduction persists for several months. Furthermore, we demonstrate that this interaction may play a substantial role at the population level. Finally, we show that the impact of LAIV on RSV burden is likely to be highly dependent on the circulation patterns of both viruses.

Results

Influenza and RSV epidemic patterns are consistent from year to year in Hong Kong

We analyzed weekly data on 1) the number and rate of samples testing positive for influenza A(H1N1), influenza B, and RSV, and 2) the proportion of influenza-like illness (ILI), defined as fever with cough or sore throat[24], per all-cause consultation in Hong Kong over several years. Due to the presence of multi-peak epidemics, which are challenging to describe using simple models, we did not consider interactions with influenza A(H3N2) (Supplementary Figure 1). After removing seasons with fewer than two thousand laboratory-confirmed influenza cases, we were left with five seasons for each virus-virus pair (influenza A(H1N1)-RSV and influenza B-RSV). Despite Hong Kong's subtropical climate, epidemics of influenza typically followed a clear seasonal pattern, with a single peak occurring during the winter or spring of each year (Figure 1a). Epidemics of RSV displayed weaker seasonality, with less definite peaks and more persistent circulation throughout the year. In most years there was considerable overlap of influenza and RSV activity, although peak activity for influenza typically preceded peak

activity for RSV. The total percentage of samples testing positive for each virus was similar for all three viruses, although season-to-season attack rates were more variable for influenza than for RSV (Supplementary Table 1).

Peak ILI activity often coincided with influenza and RSV activity, although the data were noisier (Figure 1c). This is likely due to ILI being a nonspecific, symptomatic measure that can be caused by a wide array of pathogens.

There exists a strong, negative, and bidirectional interaction between influenza and RSV, with duration of several months

To characterize the strength and duration of the interaction between influenza and RSV, we fit a deterministic, compartmental model of influenza and RSV cocirculation (Figure 2) to the data described above. We modeled the interaction effect as a decrease in the susceptibility to infection with one virus that occurs during infection with the other virus and that persists for some time after recovery. We fit the model to all available seasons for a given virus-virus pair simultaneously, such that parameters describing the interaction effect were constrained to take the same value in all seasons, whereas several season-specific parameters were allowed to vary between seasons. Confidence intervals were obtained using a parametric bootstrap[25]. A description of all model parameters can be found in Table 1, and full model equations can be found in Supplementary Equation 1. All model fitting was conducted using a maximum likelihood approach. More details on how models were fit can be found in the Methods and the Supplementary Methods.

We find that, among those currently or recently infected with influenza A(H1N1), susceptibility to RSV is reduced by almost 100% ($\theta_{\lambda 1}$ = 0; 99% CI: 0-0.02), and that this reduction in susceptibility persists for 111 days (99% CI: 96-127 days) (Table 1). We find

comparable estimates for the strength of the effect of RSV on susceptibility to A(H1N1) ($\theta_{\lambda 2}$ = 0; 99% CI: 0-0.11)). However, the duration of this effect was found to be considerably shorter than that of the effect of influenza on RSV (52 days; 99% CI: 41-72 days).

The inferred strength of the effect of influenza B on RSV was broadly similar to that of influenza A(H1N1) ($\theta_{\lambda 1}$ = 0; 99% CI: 0-0.12), although the duration of the interaction effect was somewhat shorter (89 days; 99% CI: 66-98 days). Unlike with the A(H1N1)-RSV virus-virus pair, however, the effect of RSV on influenza B appears to be unidentifiable: the confidence interval for d_2, the relative rate of loss of cross-protection against influenza after RSV, in particular, suggests a high degree of uncertainty, with the possible duration of the interaction ranging from negligible to lasting several years. Furthermore, the wide confidence interval found for $\theta_{\lambda 2}$ indicates that even the strength of the interaction during RSV infection is uncertain. Notably, these results do not necessarily signal that RSV has no impact on susceptibility to influenza B; rather, if this effect exists, it cannot be identified using this particular dataset.

To assess the role that these interactions play at the population level, we simulated epidemics at the maximum likelihood estimate (MLE) in the absence of an interaction effect. We predicted that RSV epidemics would be on average 49% larger (range across seasons: 20% to 62%) if influenza A(H1N1) did not affect RSV susceptibility, and 36% larger (range: 9% to 65%) if influenza B did not affect RSV susceptibility. Meanwhile, attack rates of influenza A(H1N1) would be on average 14% larger (range: 6% to 21%) if RSV had no impact on influenza susceptibility (Supplementary Figure 8). Overall, our results suggest that the negative interaction between influenza and RSV acts to noticeably limit the yearly attack rates of both viruses.

Both temperature and absolute humidity modulate the dynamics of influenza and RSV

Optimal model fit was achieved when both temperature and absolute humidity were included in our model (Supplementary Table 3), suggesting that temperature and absolute humidity both contribute significantly to transmission dynamics in Hong Kong. Our results suggest that transmission rates of both influenza A(H1N1) and RSV are negatively influenced by temperature when controlling for absolute humidity, and positively influenced by absolute humidity when controlling for temperature (Table 1). The impact of temperature appears to be slightly stronger for RSV than for A(H1N1), while the impact of absolute humidity is similar for both viruses. In contrast, we found little evidence that either temperature or absolute humidity plays a substantial role in driving transmission of influenza B, with only temperature showing a very small positive effect. Encouragingly, estimates of the strength of climate forcing for RSV are broadly consistent whether we model RSV alongside influenza A(H1N1) or influenza B, providing some degree of confidence that the directions of these estimates at least are correctly inferred.

Inferred reproductive numbers and immune fractions are similar across viruses but highly variable between seasons

In addition to the parameters discussed above, we also fit several season-specific parameters, including the effective reproductive numbers (*Ri1* and *Ri2*) and the proportion of the population immune to influenza (*R10* + *R120*) and RSV (*R20* + *R120*) at the beginning of each season (Table 1 and Supplementary Figure 3). The season-specific MLEs of the effective reproductive numbers for influenza ranged from 1.35 to 1.73 for influenza A(H1N1), and from 1.25 to 1.52 for influenza B. Estimates for RSV were slightly more variable, ranging from 1.16 to 1.97 when RSV was fit alongside influenza A(H1N1), and from 1.16 to 1.67 when RSV was fit alongside influenza B. Estimates of Ri2 by season differed slightly depending on which influenza (sub)type was being fit, but overall patterns were consistent.

We find that immunity to influenza and RSV is highly dependent on the season. Specifically, the season-specific percentage of the population with immunity to influenza A(H1N1) at the beginning of a season ranged from 33.2% to 89.9%, while immunity to influenza B ranged from 27.6% to 82.5%. The range of values inferred for RSV was similar, ranging from 24.5% to 74.5% of the model population when fit alongside influenza A(H1N1), and from 0% to 71.0% when fit alongside influenza B.

The best-fitting models achieve high-quality fit to data on interacting pathogens

The predicted case counts simulated from the fitted model at the MLE are highly correlated with the observed data (Figure 3), indicating that the fit model is capable of accurately reproducing observed epidemic patterns. The quality of the model fit is comparable for influenza A(H1N1) (overall R^2 = 0.93, range across seasons = 0.78-0.94) and influenza B (overall R^2 = 0.95, range = 0.78-0.96), but lower for RSV (overall R^2 = 0.67, range = 0.23-0.78 when fit alongside influenza A(H1N1); overall R^2 = 0.54, range = 0.17-0.71 when fit alongside influenza B). This could be due to the weaker seasonality of the RSV data (Figure 1a and Supplementary Table 1), which can be more difficult for simple models like the one used here to accurately capture. Collectively, these results support the utility of mathematical models as tools for describing the characteristics of pathogen-pathogen interactions.

Sensitivity analyses demonstrate the robustness of the results

As described in the Methods below, we conducted multiple rounds of model fitting to improve our chances of achieving convergence to the MLE. To further ensure convergence, we also calculated the profile likelihood[26] of $\theta_{\lambda 1}$ for both the A(H1N1)-RSV and influenza B-RSV virus-virus pairs. In both cases, the profile likelihoods peaked at the MLEs of $\theta_{\lambda 1}$

(Supplementary Figure 6), demonstrating that our model-fitting approach was indeed able to reach the true MLE.

Because transmission patterns of both influenza and RSV are dependent on age[27–29], it is possible that an age-structured model would improve the estimation of interaction characteristics. We, therefore, conducted a sensitivity analysis to evaluate whether our model, which assumes homogeneous mixing, was capable of accurately inferring interaction parameters from data derived from an age-structured population. Briefly, we generated synthetic data for all seasons at the MLE for A(H1N1)-RSV using an age-structured model, and fit our homogeneous mixing model to these data (see Supplementary Methods). Fitted values of all shared parameters agreed closely with the values used to generate the data, suggesting that our model is capable of achieving the goals outlined in this work.

Vaccination against influenza can mitigate RSV epidemics, but correct timing is critical

There is a wealth of evidence suggesting that some vaccines, especially live vaccines, can lead to temporary, nonspecific protection against non-target pathogens, likely through upregulation of the innate immune system[30,31]. Although the potential for LAIV to offer such cross-protection has not been widely studied, one study demonstrated that LAIV was able to reduce RSV replication in mice[18], and several studies have shown upregulation of the innate immune system after vaccination with LAIV[31]. If LAIV can indeed offer protection against RSV, we might expect widespread use of LAIV to reduce the population-level burden of RSV. On the other hand, given the negative interaction between influenza and RSV, a reduced burden of influenza due to widespread LAIV use could lead to inadvertent increases in the burden of RSV. To assess which of these competing effects is expected to dominate during realistic epidemics, we simulated the effect of LAIV administration, assuming imperfect or “leaky” immunity[32], at several time points and coverage levels on RSV attack rates. The model

equations can be found as Supplementary Equation 2, and the model schematic as Supplementary Figure 9. We modeled two scenarios: a "subtropical" scenario, where parameter values were set to their MLEs, and a "temperate" scenario, where season-specific parameters were chosen to yield epidemics with dynamics similar to those observed in temperate locations[33,34]. Furthermore, we considered a vaccine that reduced susceptibility to RSV by as much as natural influenza infection, as well as one that reduced susceptibility to RSV by only 50%.

In the "temperate" scenario, in which RSV typically peaks before influenza, we found that LAIV consistently decreased seasonal RSV attack rates when vaccination was as effective as natural influenza infection at preventing RSV and that this effect was stronger at earlier vaccination times and higher coverage levels (Figure 4a). A weaker but similar impact on RSV burden was observed at high vaccine coverage levels when vaccination reduced RSV susceptibility by 50%, while a small increase in burden was observed at lower coverage levels (Figure 4c). In the "subtropical" scenario based on circulation patterns in Hong Kong, where influenza often peaks before RSV, however, early vaccination on average led to an increase in RSV attack rates, particularly at coverage levels around 40-60% (Figure 4b, d). Reductions in RSV attack rates were only consistently observed if LAIV was delayed for several weeks and if coverage levels were relatively high. This pattern was consistent regardless of the strength of the vaccine effect, although the increase in RSV burden was marginally greater when the vaccine was less effective against RSV (Figure 4d). Thus, the average effect of LAIV on RSV burden at the population level was dependent on the typical circulation patterns of influenza and RSV. These results were broadly consistent across a range of sensitivity analyses in which the strength and duration of the vaccine effect were varied (Supplementary Figure 11). However, we note that in both scenarios, the exact impact of LAIV on RSV attack rates varied by season (Supplementary Figure 10), making our findings difficult to generalize. Altogether,

our results suggest that while utilizing LAIV to combat RSV is a valid strategy, the potential tradeoffs need to be carefully assessed for each location in which it is considered.

Discussion

In this work, we develop a general mathematical model of the cocirculation of two viruses and fit it to observed virologic and syndromic data to characterize the interaction between influenza viruses and RSV. We find that infection with influenza provides almost complete protection against infection with RSV for up to 3-4 months post-recovery and that RSV may have a similar but shorter-lived effect on susceptibility to influenza. Furthermore, we find that these individual-level effects likely have substantial implications for population-level epidemic dynamics and control by vaccination. Altogether, we provide one of the first estimates of the substantial individual- and population-level effects of the interaction between influenza and RSV and highlight the utility of a mathematical modeling approach in characterizing virus-virus interactions.

Our estimates of the strength and direction of the impact of influenza infection on susceptibility to RSV are consistent with past experimental work[12,13]. Furthermore, simulations in the absence of an interaction effect confirm that this interaction can have a substantial impact on RSV circulation at the population level, as possibly observed during the 2009 influenza pandemic[16,17]. Our estimate of the duration of this effect, however, was longer than expected based on earlier experimental studies. An experimental study in ferrets suggested that protection against RSV was short-lived, and that susceptibility returned to baseline levels soon after the clearance of influenza[12]. Furthermore, a past experiment in mice suggested that the upregulation of proteins involved in the interferon response, which is typically short-lived, played an important role in driving the interaction effect[13]. In contrast, we found that the interaction effect persisted for several months post-infection. These findings are consistent with

the process of "trained immunity," in which infection or vaccination yields epigenetic changes to the innate immune system. These changes in turn manifest as long-lived, nonspecific innate immune memory, and can lead to faster and more effective responses to subsequent infections. An experimental study in mice confirmed that infection with influenza was able to induce trained immunity, leading to protection against *S. pneumoniae* one month later[35]. Despite being a mechanism of the innate immune system, trained immunity in humans can persist for three months to over a year[36]. Because influenza and RSV are not closely related, we expect any interaction between them to be driven by such innate mechanisms, rather than by adaptive immunity.

In addition to the expected interaction effect of influenza on RSV, our results suggest that infection with RSV may lead to a similar reduction in susceptibility to influenza, albeit with a shorter duration. This was not expected based on existing research: while ferrets and mice infected with RSV experienced less severe illness due to influenza, they were not less likely to acquire influenza infection[12,15]. It is worth noting that much of the work on this interaction to date has focused on the effect that infection with influenza has on RSV, and not on the effect of RSV infection on influenza. Our results indicate a need for more consideration of this direction as well. While the population-level impact of RSV circulation on influenza epidemics was considerably smaller than that of influenza on RSV in this population, it may be larger in populations where RSV epidemics are larger or regularly precede influenza epidemics. Using data from Hong Kong, the individual-level effect of RSV on susceptibility to influenza was more difficult to infer than that of influenza on RSV: when influenza B and RSV were modeled together, the strength and duration parameters were unidentifiable. It is possible that modeling the interaction using data from temperate regions, where RSV epidemics tend to occur earlier in the year than influenza epidemics, may improve the model's ability to

characterize this effect. Obtaining and including data on additional seasons may also improve identifiability[20].

We are aware of only one other study using mathematical modeling methods to characterize the interaction between influenza and RSV. Waterlow et al.[23] fit a model to influenza and RSV hospitalization data from Vietnam and found that the data were equally consistent with primary infection leading to a 41% reduction in susceptibility to the other virus persisting for 10 days post-infection, and with no effect on susceptibility. While our findings are qualitatively consistent with the former result, our estimates quantitatively differ. This inconsistency may be explained by the different assumptions and components of these two models. First, in Waterlow's model, it was assumed that all individuals were susceptible to RSV at the beginning of every season, a strong assumption that may have biased the estimates of interaction. In contrast, we avoided this arbitrary assumption by estimating the initial conditions at the beginning of every season, finding strong statistical evidence against the hypothesis of full susceptibility in our data (Supplementary Figure 11). Although immunity conferred by RSV infection is imperfect, our estimates are consistent with those of a previous modeling study, which estimated a slow rate of waning immunity after RSV infection (5–15% per year in individuals aged ≥5 yr)[37]. Second, unlike Waterlow et al., we incorporated environmental variables (temperature and absolute humidity) and modeled their impact on influenza and RSV transmission. Hence, the absence of these confounders in Waterlow et al.'s model may have also biased their estimates of interactions. Finally, we allowed, and found evidence, for a non-symmetric interaction between influenza and RSV. In contrast, Waterlow et al. considered only symmetric interactions, which may not appropriately characterize the influenza-RSV system (as experimental evidence also suggests[12]).

We also report evidence that both temperature and absolute humidity play an important role in driving the transmission of both influenza and RSV. Past findings indicate that influenza

transmission increases monotonically with decreasing temperature and that there is a U-shaped relationship between transmission and absolute humidity, such that transmission increases when absolute humidity is either low or very high[38,39]. Meanwhile, RSV transmission appears to increase with lower absolute humidity and higher precipitation[41]. Given that temperature and absolute humidity are highly correlated, it makes sense that we find a reduction in the transmissibility of influenza A(H1N1) and RSV as temperatures increase, and an increase in the transmissibility of both viruses with increasing absolute humidity when controlling for temperature. The high values of absolute humidity observed year-round in Hong Kong may also explain the positive inferred effect of humidity. Although the exact estimates of climate impact on RSV transmission vary slightly depending on whether RSV is modeled alongside influenza A(H1N1) or influenza B, perhaps due to the lower-quality model fit for RSV (Figure 3b, d), we emphasize that the direction at least is consistent. Our results, therefore, contribute to the existing evidence that climate drivers of RSV, which have not been extensively studied, are similar to those for influenza A[41]. In contrast to influenza A(H1N1), we find little evidence of an impact of climate on the transmissibility of influenza B. This is surprising: while differences in the impact of climatic conditions may exist between (sub)types, we expect that all influenza (sub)types will be influenced by climate to some extent[42,43]. However, to our knowledge, the majority of past experimental work on the climate drivers of influenza has been conducted on influenza A; our results suggest that more work is needed to determine whether the same results truly hold for influenza B.

Broadly, our estimates of the season-specific reproduction numbers of both influenza and RSV are consistent with values reported in the literature[44,45]. Evaluating our results concerning the proportion immune at the beginning of each season is more challenging, as information on these parameters is less common. However, our estimates for influenza are mostly in line with findings from past modeling studies, although for some seasons we find

relatively high levels of protection[46,47]. Meanwhile, our finding of moderate to high population-level immunity to RSV is consistent with high seroprevalence among most age groups[48,49], and may in part reflect the existence of partial immunity among those with previous exposure to RSV[50,51]. Overall, the high seasonal variability in estimates of all season-specific parameters underscores the importance of fitting these parameters separately for each season, rather than assuming a constant value over time.

Given the substantial reduction in susceptibility to RSV after infection with influenza, vaccination with LAIV, which may induce similar protective effects[18], is a potentially attractive strategy for reducing RSV burden. We find that the overall impact of LAIV on RSV attack rates is highly dependent on the underlying epidemic dynamics in a population. When epidemics follow patterns typical of temperate regions, where RSV epidemics typically peak before influenza epidemics, widespread use of LAIV tends to reduce RSV burden. However, in epidemics following patterns typical of Hong Kong, where influenza epidemics occur before or simultaneously with RSV epidemics, LAIV tends to increase RSV burden unless vaccination is delayed for several weeks. Vaccines with a stronger individual-level effect on RSV susceptibility yielded a more beneficial (in temperate regions) and less detrimental (in the subtropics) outcome at the population level, although this pattern was not always consistent across seasons (Supplementary Figure 10). Our findings are consistent with previous work on influenza vaccines: during the 2009 influenza pandemic, observational studies in Canada reported an increase in the odds of infection with H1N1pdm09 among those vaccinated against seasonal influenza[9], while a randomized controlled trial of influenza vaccine found higher rates of non-influenza infections among vaccinated children[10]. Both observations were suggested to have been driven by a lack of temporary, nonspecific immunity among those who were vaccinated, resulting from lower levels of natural infection with seasonal influenza. Since influenza is particularly dangerous in exactly those age groups most affected by RSV[11], it is

unlikely that the increased influenza burden that would result from delaying vaccination until later in the season represents an appropriate public health tradeoff. Future studies could assess in more detail how to best balance these competing effects. Additionally, future work is necessary to determine the actual impact of LAIV on RSV risk at the individual level: while LAIV has been shown to have a protective effect against RSV in mice[18], no studies to date have assessed the strength and duration of its impact on RSV susceptibility in humans.

It is therefore difficult to make generalizations concerning the public health potential of LAIV to reduce RSV burden. Instead, the benefits and drawbacks of using LAIV to control RSV should be carefully considered for each separate location in which this strategy is proposed. However, it is encouraging to find that, in some regions, LAIV could lead to substantial reductions in RSV attack rates while we await approval of vaccines against RSV. More generally, our results pave the way for future work on the indirect effects of vaccines, a topic that has received increasing attention throughout the COVID-19 pandemic[52,53].

Broadly, the results of this simulation study also highlight the importance of accounting for interactions between pathogens when conducting research on infectious diseases. Although interactions are understudied, they are likely to represent a prominent element of infectious disease epidemiology. In addition to influenza and RSV, interactions of public health relevance likely exist between influenza viruses and *S. pneumoniae*[7,8], influenza and rhinovirus[3,54], and influenza and SARS-CoV-2[55], among many others. As we have demonstrated, failure to account for these interaction effects could lead to considerable over- or underestimates of the effects of proposed public health strategies. In more extreme scenarios, the implementation of ineffective or even harmful interventions could be detrimental not only to public health but also to public perception of infectious disease epidemiology and of modeling, fields which already suffer from a lack of trust from the public[56–59]. Where polymicrobial systems made up

of interacting pathogens exist, studying individual pathogens in isolation will not be sufficient to guide informed public health planning.

Of course, to effectively account for interactions in public health practice, researchers and practitioners alike will require a better understanding of these interactions. Our work demonstrates that mathematical modeling methods can be instrumental in achieving this understanding. While not all parameters were identifiable for all virus-virus pairs, our model was generally able to infer the characteristics of interaction effects with high precision. This was true despite the large number of parameters (47 for each virus-virus pair) we attempted to estimate. Furthermore, a past simulation study showed that interactions can be difficult to properly infer when they are short-lived, or when data are not available for a large number of seasons[20]. However, here we can estimate the strength and duration of a relatively short-term interaction with only five seasons of data. Since the influence of interactions can be difficult or even impossible to discern using standard observational epidemiologic methods[6,20], it is particularly encouraging to find that transmission models can be successful where other methods fail. Critically, transmission models explicitly and mechanistically account for all components of interaction, something that purely statistical methods are not capable of achieving. Of course, these methods will not always be effective, and identifiability issues may persist depending on the data used. Our data did not allow for the effect of RSV on influenza B to be estimated, and a previous modeling study found that the impact of influenza on susceptibility to RSV could not be inferred using data from Vietnam[23]. In particular, challenges in correctly inferring the characteristics of interactions between two pathogens may arise in locations where the overlap between circulating pathogens is low, or where one pathogen consistently peaks before the other. By applying mathematical modeling methods to data from other locations, future work can explore which epidemic features make interaction parameters easier or more difficult to precisely infer. Meanwhile, synthetic data generated from our

empirically-validated model can be used to assess new statistical methods for inferring interaction characteristics, an approach similar to that used in[6].

Despite our promising findings, several limitations of this study are worth noting. First, our model does not include age structure and instead assumes homogeneous mixing throughout the population. As children are expected to contribute disproportionately to the transmission of both influenza and RSV[27–29], it might be expected that interaction effects would be easier to estimate in an age-structured model, where the impact of the interaction would be more concentrated in those age groups with higher attack rates. To assess this directly, we generated synthetic epidemic data from an age-structured model, and fit our model to these data. We found that the homogeneous mixing model was able to correctly infer the values of the interaction parameters, perhaps because the synthetic epidemics were synchronous across age groups (Supplementary Figure 12). This suggests that homogeneous models are sufficient to capture the broad characteristics of this interaction, even when the underlying transmission dynamics vary by age group (see Supplementary Methods). This is encouraging, as the large number of unknown parameters (including initial conditions) in age-structured models makes their estimation challenging.

A second limitation is that we do not consider the potential impact of the interaction effect on disease severity, choosing to focus solely on the effect on susceptibility. Past research has yielded mixed results concerning the severity of coinfections with influenza and RSV: some studies have found coinfections to be more severe than infections with either virus alone[60,61], while others have found evidence of reduced severity[12,15]. In the modeling study of influenza and RSV cocirculation in Vietnam discussed above, the fitted model was most consistent with a 2-20 times increase in reporting among coinfected individuals[23]. We attempted to fit our model allowing for a change in infection severity among coinfected individuals but found that this effect was not identifiable. This suggests that we have reached

the limit of what our particular combination of data and model can infer about the interaction between influenza and RSV, but it is important that future work, perhaps using data from several locations, continue to explore this effect. Encouragingly, including an effect on severity in our model did not alter the MLEs of the other shared model parameters, suggesting that our results regarding the interaction effect on susceptibility were not compromised by not including an effect on severity.

Third, our use of a relatively simple model best-suited to reproducing unimodal epidemics precluded the inclusion of influenza A(H3N2) in this study. While we would expect the effect of A(H3N2) on RSV to be similar to that of other influenza (sub)types, which demonstrated similar effects on susceptibility to RSV in this work, future work will assess this directly by developing a more complicated model of multi-peak seasonal epidemics. Such a model would also allow for the study of interactions with additional pathogens typically associated with multiple peaks or year-round transmission. For example, rhinovirus tends to peak in both spring and autumn and may reduce replication and onward transmission of influenza[54,63]. Hence, extending the model presented here to consider alternative pairs, or a greater number, of respiratory viruses, is an exciting area for future research.

As a final limitation, we note that we focus here on a single location, Hong Kong. This was due in large part to limitations in available data. While virologic data on influenza are fairly widely available, far fewer countries conduct routine surveillance for RSV[64]. High-quality data on ILI rates are similarly difficult to acquire[46]. Improvements in data collection and reporting are urgently needed to allow this type of work in a variety of settings. As mentioned above, including data from multiple locations would be instrumental in improving our understanding of which epidemic patterns allow for the precise estimation of interaction parameters, and which render these parameters difficult or impossible to infer. In cases where estimation of parameter values proves challenging, compiling data from multiple locations

could also improve identifiability: as we expect interactions to display the same strength and duration on the individual level regardless of location, models could be fit to data from several regions simultaneously to find those parameter estimates most consistent with epidemic dynamics across locations.

Conclusions

In this work, we produce one of the first estimates of the strength and duration of the interaction between influenza viruses and RSV, and of the relevance of this interaction in modulating disease burden. Specifically, we show that infection with either influenza virus or RSV causes a temporary but strong reduction in susceptibility to the other virus and that this individual-level effect can lead to substantial ramifications at the population level. We further explore the implications of this finding for a novel RSV control strategy and find that the effect of vaccination with LAIV at the population level is highly dependent on the underlying transmission dynamics of both viruses in a given location. Overall, our results demonstrate that accounting for pathogen-pathogen interactions is critical, both when conducting epidemiologic research and when formulating practical strategies to reduce the burden of infectious diseases. Furthermore, we show that mathematical models are a powerful tool for improving our understanding of how these interactions operate at the individual- and population-levels.

Methods

Respiratory Infection Data

Weekly data on influenza and RSV circulation in Hong Kong from 2014 through 2019 were obtained from the Centre for Health Protection of the Government of the Hong Kong Special Administrative Region[65]. These data consisted of the number of samples testing positive for influenza and RSV, as well as the total number of samples tested (Figure 1a-b). Influenza virus

detections were broken down by type (A or B) and by subtype (for influenza A viruses). Samples were obtained from outpatient clinics and public hospitals, and all testing from February 10, 2014, was done using molecular testing rather than viral culture[39]. We also obtained data on the weekly proportion of all consultations that were due to influenza-like illness (ILI) within a sentinel surveillance network of public out-patient clinics from the same source[66] (Figure 1c).

We separated the data into seasons, such that seasons began in week 46 (mid-November) and continued through week 45 of the following year. This cutoff was chosen as earlier cutoffs often occurred mid-RSV epidemic, while later cutoffs were prone to occur during influenza epidemics. Because epidemics of influenza A(H3N2) often displayed multiple peaks per year, we do not consider influenza A(H3N2) here. We were therefore left with six seasons of data (2013-14 through 2018-19) for two virus-virus pairs (influenza A(H1N1)-RSV, and influenza B-RSV). Although data were not available for 2013, and therefore for the first seven weeks of the 2013-14 season, we retained this season in our dataset to maximize the number of seasons available for analysis. For each virus-virus pair, fitting was only performed for those seasons where greater than 2000 influenza cases were reported, as the impact of a virus-virus interaction is expected to be minimal in the absence of substantial circulation of both viruses.

Transmission Model

We represent the transmission of influenza and RSV throughout the model population using a deterministic, compartmental SITRxSITR model, in which compartments indicate the infection status of individuals according to both viruses (e.g., X_SI represents the number of people susceptible to influenza and infected with RSV). This results in a total of sixteen compartments (Figure 2). The interaction effect is modeled by reducing the force of infection of one virus

among those currently (I) or recently (T) infected with the other virus (i.e., the interaction operates by reducing susceptibility to infection). Both the strength (i.e., the extent of this reduction) and duration (i.e., the amount of time spent in compartment T) of the interaction are allowed to vary according to whether an individual is initially infected with influenza or with RSV (i.e., the interaction is allowed to be asymmetric). This model is comparable to the one initially developed by Shrestha et al.[20].

Because we model each yearly epidemic separately, we assume no within-season waning immunity. This assumption is in line with estimates of the duration of immunity for both influenza and RSV. Immunity to influenza is consistently estimated to last for multiple years[67,68]. While estimates for RSV are less certain, past modeling work has suggested that immunity persists for at least one year[37,69]. Furthermore, our assumption is consistent with other RSV modeling work, which also does not account for within-season waning of immunity[23,70].

Average infectious periods were fixed at 5 days for influenza[71] and 10 days for RSV[72,73]. The size of the model population is taken to be the population size of Hong Kong during each epidemic, based on data from the Census and Statistics Department of the Government of the Hong Kong Special Administrative Region[74].

Climate Forcing

Evidence suggests that climatic conditions act as important drivers of influenza and RSV transmission. Specifically, a U-shaped effect of absolute humidity on influenza transmission has been suggested, with higher transmission occurring when humidity is either low or very high[38,39]. The effect of temperature, meanwhile, is monotonic, such that increased transmission occurs at lower temperatures[38–40]. Although RSV has received less attention, existing work suggests that temperature and humidity modulate RSV transmission in a similar manner[41,75].

Here, we allow the force of infection for each virus to vary according to an exponential function of weekly average mean temperature and absolute humidity, such that:

$$\beta_i(t) = \widehat{\beta_i} e^{\eta_{AH_i} AH(t) + \eta_{temp_i} T(t)} \quad (1)$$

where η_{temp1} and η_{AH1} represent the extent to which temperature and absolute humidity, respectively, impact the transmissibility of influenza, and η_{temp2} and η_{AH2} represent the extent to which temperature and absolute humidity, respectively, impact the transmissibility of RSV; $\widehat{\beta_1}$ and $\widehat{\beta_2}$ represent the force of infection of influenza and RSV in the absence of climate forcing. Although we do not expect the effect of absolute humidity to be monotonic based on past studies[38,39], we choose to model the relationship with a monotonic, exponential function for simplicity. We believe this simplification makes sense because (1) absolute humidity in Hong Kong is high year-round (Supplementary Figure 2b), likely rendering the effect of low absolute humidity less important, and (2) temperate and absolute humidity are highly correlated (Supplementary Figure 2c), such that we may expect transmissibility to increase monotonically with absolute humidity once temperature is controlled for.

Daily mean temperature and relative humidity data were obtained from the US National Centers for Environmental Information's Global Surface Summary of the Day (GSOD) data using the R package GSODR[76,77], and absolute humidity was calculated using the Clausius-Clapeyron relation[78]. Weekly values were taken to be the mean values of temperature and absolute humidity each week. Finally, data were standardized to have a mean of zero and a variance of one. This was done both to convert the climate data into a dimensionless form, and to facilitate interpretation of the climate forcing parameters.

Because temperature and absolute humidity are highly correlated (Pearson's r = 0.944 over the course of the study period; see Supplementary Figure 2), we performed a sensitivity

analysis to check whether including both variables improved model fit over including temperature alone.

Observation Model

Due to the prevalence of mild and asymptomatic infections, many cases of influenza and RSV are never reported, and therefore do not show up in empirical datasets. To model the process by which individuals seek healthcare and are tested for specific viral infections, we draw from a binomial distribution at each time point, where the number of trials is equal to the total observed number of tests for respiratory viruses conducted that week, and the probabilities of a positive test for influenza ($\rho_1(t)$) or RSV ($\rho_2(t)$) are:

$$\rho_i(t) = \left(1.0, \rho_i\left(1.0 + \alpha \cos\cos\left(\frac{2\pi}{52.25}(t-\phi)\right)\right)\frac{H_i(t)}{ILI(t)}\right) \quad (2)$$

Here, $H_i(t)$ represents the modeled incidence of virus i at time t, while $ILI(t)$ represents the observed proportion of ILI per consultation in Hong Kong at time t. The parameter ρ_i is a composite reporting rate and scaling parameter for virus i, and allows for a direct comparison to be made between the modeled output and the data [46,79] (see Supplementary Methods). We account for possible seasonality in reporting and background consultation rates using a cosine function, where α represents the amplitude of this seasonality, and φ represents the time at which ρ_i is maximal.

Model Fitting

For model fitting, parameters are designated as either shared or season-specific (Table 1). Shared parameters (e.g., those describing interaction characteristics or climate forcing) are assumed not to vary by season, and are therefore constrained to take the same value in all

seasons for a given virus-virus pair; season-specific parameters (e.g., the initial reproductive number or the proportion immune at the start of the season) are allowed to differ by season.

All model fitting was accomplished using a maximum likelihood approach to conduct trajectory matching. More specifically, model fitting was performed using a two-step process. In the first step, we obtained reasonable initial estimates for the season-specific parameters by fitting each season of data for each virus-virus pair separately, assuming no interaction, climate forcing, or reporting seasonality. In the second step, we fit the model to all seasons of data for each virus-virus pair simultaneously, with initial values of the season-specific parameters drawn from the ranges fit in the previous step. By constraining this second step to begin in a relatively good region of the parameter space, we allow for more efficient convergence to the MLE. To ensure convergence to the MLE, multiple rounds of fitting to all seasons simultaneously were performed.

We obtained 99% confidence intervals for all parameter values using parametric bootstrapping[25]. This method is computationally efficient and has been shown to perform well for similar work in the past [8,55,80]. Specifically, we generated 500 sets of synthetic epidemics at the MLE for each virus-virus pair using the stochastic observation model, where each set contained a simulated epidemic for all available seasons, and fit the model to each set of synthetic epidemics. Confidence intervals were obtained by computing the highest posterior density[81] of the best-fit estimates over all 500 synthetic epidemics. More specific details on the process used for model fitting and construction of the confidence intervals can be found in the Supplementary Methods.

We assessed the quality of model fits by comparing the observed data to data simulated from the model at the MLE. We further confirmed convergence to the MLE by calculating the profile likelihood of $\theta_{\lambda 1}$[26] (Supplementary Figure 6).

Simulation Study of Vaccine Impact

To assess the potential for vaccination with a live attenuated influenza vaccine (LAIV) to reduce the burden of RSV, we conducted a simulation study. We adapted our SITRxSITR model, described above, to allow for vaccination of individuals who were fully susceptible to influenza, RSV, or both (i.e., those in compartments X_SS, X_SI, X_ST, X_SR, or X_RS) with LAIV (Supplementary Equation 2 and Supplementary Figure S9). Vaccination was assumed to confer either the same protection against RSV as does natural influenza infection or reduced protection relative to natural infection ($\theta_{\lambda vacc}$ = 0.5); in both cases, protection against RSV due to LAIV was assumed to wane at the same rate as protection due to natural infection (see Table 1). Additionally, vaccination conferred imperfect ("leaky") immunity to influenza[32] with a vaccine efficacy of 80%[82]. For simplicity, we assume that all vaccinated individuals receive the vaccine at a single instantaneous time point.

Although influenza and RSV tend to display regular seasonal patterns in Hong Kong, epidemic dynamics still differ from those in many temperate regions. Specifically, in Hong Kong, epidemics of influenza often occurred before or simultaneously with RSV epidemics, whereas RSV epidemics tend to precede influenza epidemics in many temperate regions[83]. Thus, we ran our simulation study for two scenarios: a "subtropical" scenario, where all model parameters were set to the MLEs obtained when fitting the model to data from Hong Kong on A(H1N1) and RSV, and a "temperate" scenario, where values of *Ri1*, *Ri2*, *I10*, and *I20* were selected using Latin hypercube sampling to more closely resemble observed patterns of influenza and RSV transmission in France (see Supplementary Methods)[33,34].

For each scenario, we simulated the total number of influenza and RSV cases over the course of each season at a range of vaccine coverage levels and timings using our deterministic model. We calculated the influence of LAIV on RSV burden for each simulation as a rate ratio:

$$RR = \frac{AR_{RSV}^{1}}{AR_{RSV}^{0}} \quad (3)$$

where AR_{RSV}^{1} represents the RSV attack rate throughout the season in a partially vaccinated population, and AR_{RSV}^{0} represents the RSV attack rate in a population where no vaccination occurred. Thus, values less than one indicate that LAIV reduced the overall attack rate of RSV for the season, while values greater than one indicate that LAIV led to an increase in the attack rate of RSV. Several sensitivity analyses, where vaccine efficacy and duration were varied, were also conducted (see Supplementary Figure 11).

Implementation

Model fitting and the simulation study of vaccination were conducted in R version 4.0.2, and results were analyzed using R version 4.1.0[84]. The model was coded and run using the package pomp[85], and fit using the sbplx algorithm via the package nloptr[86,87]. All code can be found on GitHub[88], as well as on Edmond, the Open Research Data Repository of the Max Planck Society[89].

Data availability statement

All the data and R codes can be found at:

https://github.com/sarahckramer/resp_virus_interactions.

References

1. DaPalma, T., Doonan, B. P., Trager, N. M. & Kasman, L. M. A systematic approach to virus–virus interactions. *Virus Res.* **149**, 1–9 (2010).
2. Bosch, A. A. T. M., Biesbroek, G., Trzcinski, K., Sanders, E. A. M. & Bogaert, D. Viral and bacterial interactions in the upper respiratory tract. *PLoS Pathog.* **9**, e1003057 (2013).
3. Nickbakhsh, S. *et al.* Virus-virus interactions impact the population dynamics of influenza and the common cold. *Proc. Natl. Acad. Sci. U. S. A.* (2019) doi:10.1073/pnas.1911083116.
4. Wong, A. *et al.* The interactions of SARS-CoV-2 with co-circulating pathogens: Epidemiological implications and current knowledge gaps. *arXiv [q-bio.PE]* (2022).
5. Opatowski, L., Baguelin, M. & Eggo, R. M. Influenza interaction with cocirculating pathogens and its impact on surveillance, pathogenesis, and epidemic profile: A key role for mathematical modelling. *PLoS Pathog.* **14**, e1006770 (2018).
6. Domenech de Cellès, M., Goult, E., Casalegno, J.-S. & Kramer, S. C. The pitfalls of inferring virus–virus interactions from co-detection prevalence data: application to influenza and SARS-CoV-2. *Proceedings of the Royal Society B: Biological Sciences* **289**, 20212358 (2022).
7. Shrestha, S. *et al.* Identifying the interaction between influenza and pneumococcal pneumonia using incidence data. *Sci. Transl. Med.* **5**, 191ra84 (2013).
8. Domenech de Cellès, M. *et al.* Unraveling the seasonal epidemiology of pneumococcus. *Proc. Natl. Acad. Sci. U. S. A.* **116**, 1802–1807 (2019).
9. Mercer, G. N., Barry, S. I. & Kelly, H. Modelling the effect of seasonal influenza vaccination on the risk of pandemic influenza infection. *BMC Public Health* **11 Suppl 1**, S11 (2011).

10. Cowling, B. J. *et al.* Increased risk of noninfluenza respiratory virus infections associated with receipt of inactivated influenza vaccine. *Clin. Infect. Dis.* **54**, 1778–1783 (2012).
11. GBD 2016 Lower Respiratory Infections Collaborators. Estimates of the global, regional, and national morbidity, mortality, and aetiologies of lower respiratory infections in 195 countries, 1990-2016: a systematic analysis for the Global Burden of Disease Study 2016. *Lancet Infect. Dis.* **18**, 1191–1210 (2018).
12. Chan, K. F. *et al.* Investigating Viral Interference Between Influenza A Virus and Human Respiratory Syncytial Virus in a Ferret Model of Infection. *J. Infect. Dis.* **218**, 406–417 (2018).
13. Drori, Y. *et al.* Influenza A Virus Inhibits RSV Infection via a Two-Wave Expression of IFIT Proteins. *Viruses* **12**, (2020).
14. Walzl, G., Tafuro, S., Moss, P., Openshaw, P. J. M. & Hussell, T. Influenza Virus Lung Infection Protects from Respiratory Syncytial Virus–Induced Immunopathology. *J. Exp. Med.* **192**, 1317–1326 (2000).
15. Hartwig, S. M., Miller, A. M. & Varga, S. M. Respiratory Syncytial Virus Provides Protection against a Subsequent Influenza A Virus Infection. *J. Immunol.* **208**, 720–731 (2022).
16. Li, Y. *et al.* The impact of the 2009 influenza pandemic on the seasonality of human respiratory syncytial virus: A systematic analysis. *Influenza Other Respi. Viruses* **15**, 804–812 (2021).
17. Mak, G. C., Wong, A. H., Ho, W. Y. Y. & Lim, W. The impact of pandemic influenza A (H1N1) 2009 on the circulation of respiratory viruses 2009-2011. *Influenza Other Respi. Viruses* **6**, e6–10 (2012).
18. Lee, Y. J. *et al.* Non-specific Effect of Vaccines: Immediate Protection against Respiratory Syncytial Virus Infection by a Live Attenuated Influenza Vaccine. *Front.*

Microbiol. **9**, 83 (2018).

19. Mazur, N. I. *et al.* The respiratory syncytial virus vaccine landscape: lessons from the graveyard and promising candidates. *Lancet Infect. Dis.* **18**, e295–e311 (2018).
20. Shrestha, S., King, A. A. & Rohani, P. Statistical inference for multi-pathogen systems. *PLoS Comput. Biol.* **7**, e1002135 (2011).
21. Keeling, M. J. & Rohani, P. *Modeling Infectious Diseases in Humans and Animals*. (Princeton University Press, 2011).
22. Waterlow, N. R., Flasche, S., Minter, A. & Eggo, R. M. Competition between RSV and influenza: Limits of modelling inference from surveillance data. *Epidemics* **35**, 100460 (2021).
23. Waterlow, N. R. *et al.* Evidence for influenza and RSV interaction from 10 years of enhanced surveillance in Nha Trang, Vietnam, a modelling study. *PLoS Comput. Biol.* **18**, e1010234 (2022).
24. Cowling, B. J., Wong, I. O. L., Ho, L.-M., Riley, S. & Leung, G. M. Methods for monitoring influenza surveillance data. *Int. J. Epidemiol.* **35**, 1314–1321 (2006).
25. Roosa, K. & Chowell, G. Assessing parameter identifiability in compartmental dynamic models using a computational approach: application to infectious disease transmission models. *Theor. Biol. Med. Model.* **16**, 1 (2019).
26. Raue, A. *et al.* Structural and practical identifiability analysis of partially observed dynamical models by exploiting the profile likelihood. *Bioinformatics* **25**, 1923–1929 (2009).
27. Lau, M. S. Y., Cowling, B. J., Cook, A. R. & Riley, S. Inferring influenza dynamics and control in households. *Proc. Natl. Acad. Sci. U. S. A.* **112**, 9094–9099 (2015).
28. Viboud, C. *et al.* Risk factors of influenza transmission in households. *Br. J. Gen. Pract.* **54**, 684–689 (2004).

29. Goldstein, E. *et al.* On the Relative Role of Different Age Groups During Epidemics Associated With Respiratory Syncytial Virus. *J. Infect. Dis.* **217**, 238–244 (2018).
30. Aaby, P., Kollmann, T. R. & Benn, C. S. Nonspecific effects of neonatal and infant vaccination: public-health, immunological and conceptual challenges. *Nat. Immunol.* **15**, 895–899 (2014).
31. Blok, B. A., Arts, R. J. W., van Crevel, R., Benn, C. S. & Netea, M. G. Trained innate immunity as underlying mechanism for the long-term, nonspecific effects of vaccines. *J. Leukoc. Biol.* **98**, 347–356 (2015).
32. Elizabeth Halloran, M., Longini, I. M., Jr & Struchiner, C. J. *Design and Analysis of Vaccine Studies*. (Springer New York, 2009).
33. Mosnier, A. *et al.* Ten influenza seasons in France: distribution and timing of influenza A and B circulation, 2003-2013. *BMC Infect. Dis.* **15**, 357 (2015).
34. GROG (Groupes Régionaux d'Observation de la Grippe). http://www.grog.org/ (2020).
35. Aegerter, H. *et al.* Influenza-induced monocyte-derived alveolar macrophages confer prolonged antibacterial protection. *Nat. Immunol.* **21**, 145–157 (2020).
36. Netea, M. G. *et al.* Defining trained immunity and its role in health and disease. *Nat. Rev. Immunol.* **20**, 375–388 (2020).
37. van Boven, M. *et al.* Estimating Transmission Parameters for Respiratory Syncytial Virus and Predicting the Impact of Maternal and Pediatric Vaccination. *J. Infect. Dis.* **222**, S688–S694 (2020).
38. Deyle, E. R., Maher, M. C., Hernandez, R. D., Basu, S. & Sugihara, G. Global environmental drivers of influenza. *Proc. Natl. Acad. Sci. U. S. A.* **113**, 13081–13086 (2016).
39. Yuan, H., Kramer, S. C., Lau, E. H. Y., Cowling, B. J. & Yang, W. Modeling influenza seasonality in the tropics and subtropics. *PLoS Comput. Biol.* **17**, e1009050 (2021).

40. Lowen, A. C., Mubareka, S., Steel, J. & Palese, P. Influenza virus transmission is dependent on relative humidity and temperature. *PLoS Pathog.* **3**, 1470–1476 (2007).
41. Baker, R. E. *et al.* Epidemic dynamics of respiratory syncytial virus in current and future climates. *Nat. Commun.* **10**, 5512 (2019).
42. Zhang, B. *et al.* Subtypes specified environmental dependence of seasonal influenza virus. *Sci. Total Environ.* **852**, 158525 (2022).
43. Kormuth, K. A. *et al.* Environmental Persistence of Influenza Viruses Is Dependent upon Virus Type and Host Origin. *mSphere* **4**, (2019).
44. Biggerstaff, M., Cauchemez, S., Reed, C., Gambhir, M. & Finelli, L. Estimates of the reproduction number for seasonal, pandemic, and zoonotic influenza: a systematic review of the literature. *BMC Infect. Dis.* **14**, 480 (2014).
45. Reis, J. & Shaman, J. Simulation of four respiratory viruses and inference of epidemiological parameters. *Infect Dis Model* **3**, 23–34 (2018).
46. Kramer, S. C. & Shaman, J. Development and validation of influenza forecasting for 64 temperate and tropical countries. *PLoS Comput. Biol.* **15**, e1006742 (2019).
47. Yang, W., Cowling, B. J., Lau, E. H. Y. & Shaman, J. Forecasting Influenza Epidemics in Hong Kong. *PLoS Comput. Biol.* **11**, e1004383 (2015).
48. Cox, M. J., Azevedo, R. S., Cane, P. A., Massad, E. & Medley, G. F. Seroepidemiological study of respiratory syncytial virus in São Paulo state, Brazil. *J. Med. Virol.* **55**, 234–239 (1998).
49. Lu, G. *et al.* Large-scale seroprevalence analysis of human metapneumovirus and human respiratory syncytial virus infections in Beijing, China. *Virol. J.* **8**, 62 (2011).
50. White, L. J. *et al.* Understanding the transmission dynamics of respiratory syncytial virus using multiple time series and nested models. *Math. Biosci.* **209**, 222–239 (2007).
51. Henderson, F. W., Collier, A. M., Clyde, W. A., Jr & Denny, F. W. Respiratory-

syncytial-virus infections, reinfections and immunity. A prospective, longitudinal study in young children. *N. Engl. J. Med.* **300**, 530–534 (1979).

52. Upton, C. M. *et al.* Safety and efficacy of BCG re-vaccination in relation to COVID-19 morbidity in healthcare workers: A double-blind, randomised, controlled, phase 3 trial. *EClinicalMedicine* **48**, 101414 (2022).
53. Fink, G. *et al.* Inactivated trivalent influenza vaccination is associated with lower mortality among patients with COVID-19 in Brazil. *BMJ Evid Based Med* (2020) doi:10.1136/bmjebm-2020-111549.
54. Wu, A., Mihaylova, V. T., Landry, M. L. & Foxman, E. F. Interference between rhinovirus and influenza A virus: a clinical data analysis and experimental infection study. *Lancet Microbe* **1**, e254–e262 (2020).
55. Domenech de Cellès, M., Casalegno, J.-S., Lina, B. & Opatowski, L. Estimating the impact of influenza on the epidemiological dynamics of SARS-CoV-2. *PeerJ* **9**, e12566 (2021).
56. Larson, H. J., Jarrett, C., Eckersberger, E., Smith, D. M. D. & Paterson, P. Understanding vaccine hesitancy around vaccines and vaccination from a global perspective: a systematic review of published literature, 2007-2012. *Vaccine* **32**, 2150–2159 (2014).
57. Al-Ramahi, M., Elnoshokaty, A., El-Gayar, O., Nasralah, T. & Wahbeh, A. Public Discourse Against Masks in the COVID-19 Era: Infodemiology Study of Twitter Data. *JMIR Public Health Surveill* **7**, e26780 (2021).
58. Alwan, N. A. *et al.* Evidence informing the UK's COVID-19 public health response must be transparent. *Lancet* **395**, 1036–1037 (2020).
59. Enserink, M. & Kupferschmidt, K. With COVID-19, modeling takes on life and death importance. *Science* **367**, 1414–1415 (2020).
60. George, J. A., AlShamsi, S. H., Alhammadi, M. H. & Alsuwaidi, A. R. Exacerbation of

Influenza A Virus Disease Severity by Respiratory Syncytial Virus Co-Infection in a Mouse Model. *Viruses* **13**, (2021).

61. Zhang, Y. *et al.* Severity of influenza virus and respiratory syncytial virus coinfections in hospitalized adult patients. *J. Clin. Virol.* **133**, 104685 (2020).
62. Monto, A. S. The seasonality of rhinovirus infections and its implications for clinical recognition. *Clin. Ther.* **24**, 1987–1997 (2002).
63. Linde, A., Rotzén-Ostlund, M., Zweygberg-Wirgart, B., Rubinova, S. & Brytting, M. Does viral interference affect spread of influenza? *Euro Surveill.* **14**, (2009).
64. Campbell, H., Bont, L. & Nair, H. Respiratory syncytial virus (RSV) disease - new data needed to guide future policy. *J. Glob. Health* **5**, 020101 (2015).
65. Centre for Health Protection. Detection of pathogens from respiratory specimens. *chp.gov.hk* https://www.chp.gov.hk/en/statistics/data/10/641/642/2274.html (2022).
66. Centre for Health Protection. General Out-patient Clinics / Private Medical Practitioner Clinics. *chp.gov.hk* https://www.chp.gov.hk/en/static/24015.html (2022).
67. Couch, R. B. & Kasel, J. A. Immunity to influenza in man. *Annu. Rev. Microbiol.* **37**, 529–549 (1983).
68. Ranjeva, S. *et al.* Age-specific differences in the dynamics of protective immunity to influenza. *Nat. Commun.* **10**, 1660 (2019).
69. Hodgson, D., Pebody, R., Panovska-Griffiths, J., Baguelin, M. & Atkins, K. E. Evaluating the next generation of RSV intervention strategies: a mathematical modelling study and cost-effectiveness analysis. *BMC Med.* **18**, 348 (2020).
70. Reis, J. & Shaman, J. Retrospective Parameter Estimation and Forecast of Respiratory Syncytial Virus in the United States. *PLoS Comput. Biol.* **12**, e1005133 (2016).
71. Carrat, F. *et al.* Time lines of infection and disease in human influenza: a review of volunteer challenge studies. *Am. J. Epidemiol.* **167**, 775–785 (2008).

72. Munywoki, P. K. *et al.* Influence of age, severity of infection, and co-infection on the duration of respiratory syncytial virus (RSV) shedding. *Epidemiol. Infect.* **143**, 804–812 (2015).

73. Moore, H. C., Jacoby, P., Hogan, A. B., Blyth, C. C. & Mercer, G. N. Modelling the seasonal epidemics of respiratory syncytial virus in young children. *PLoS One* **9**, e100422 (2014).

74. Census and Statistics Department. Table 1A : Population by Sex and Age Group [English]. *data.gov.hk* https://www.censtatd.gov.hk/en/web_table.html?id=1A (2022).

75. Pitzer, V. E. *et al.* Environmental drivers of the spatiotemporal dynamics of respiratory syncytial virus in the United States. *PLoS Pathog.* **11**, e1004591 (2015).

76. National Centers for Environmental Information. Global Surface Summary of the Day - GSOD. *ncei.noaa.gov* https://www.ncei.noaa.gov/access/metadata/landing-page/bin/iso?id=gov.noaa.ncdc:C00516 (2022).

77. H Sparks, A., Hengl, T. & Nelson, A. GSODR: Global summary daily weather data in R. *J. Open Source Softw.* **2**, 177 (2017).

78. Wallace, J. M. & Hobbs, P. V. *Atmospheric Science: An Introductory Survey*. (Elsevier, 2006).

79. Kramer, S. C., Pei, S. & Shaman, J. Forecasting influenza in Europe using a metapopulation model incorporating cross-border commuting and air travel. *PLoS Comput. Biol.* **16**, e1008233 (2020).

80. Domenech de Cellès, M., Magpantay, F. M. G., King, A. A. & Rohani, P. The impact of past vaccination coverage and immunity on pertussis resurgence. *Sci. Transl. Med.* **10**, (2018).

81. McElreath, R. *Statistical Rethinking: A Bayesian Course with Examples in R and Stan*. (CRC Press, 2020).

82. Jefferson, T., Rivetti, A., Di Pietrantonj, C. & Demicheli, V. Vaccines for preventing influenza in healthy children. *Cochrane Database Syst. Rev.* **2**, CD004879 (2018).

83. Li, Y. *et al.* Global patterns in monthly activity of influenza virus, respiratory syncytial virus, parainfluenza virus, and metapneumovirus: a systematic analysis. *Lancet Glob Health* **7**, e1031–e1045 (2019).

84. R Core Team. R: A Language and Environment for Statistical Computing. Preprint at https://www.R-project.org/ (2021).

85. King, A. A., Nguyen, D. & Ionides, E. L. Statistical Inference for Partially Observed Markov Processes via the R Package pomp. *J. Stat. Softw.* **69**, 1–43 (2016).

86. Rowan, T. H. Functional stability analysis of numerical algorithms. (University of Texas at Austin, 1990).

87. Johnson, S. G. The NLopt nonlinear-optimization package. Preprint at http://ab-initio.mit.edu/nlopt.

88. Kramer, S. C. Respiratory Virus Interactions. Preprint at https://github.com/sarahckramer/resp_virus_interactions (2022).

89. Kramer, S. C. Code for ‘Characterizing the epidemiological interactions between influenza and respiratory syncytial viruses and their implications for disease control’. (2022) doi:10.17617/3.TBOPCK.

Figure Legends

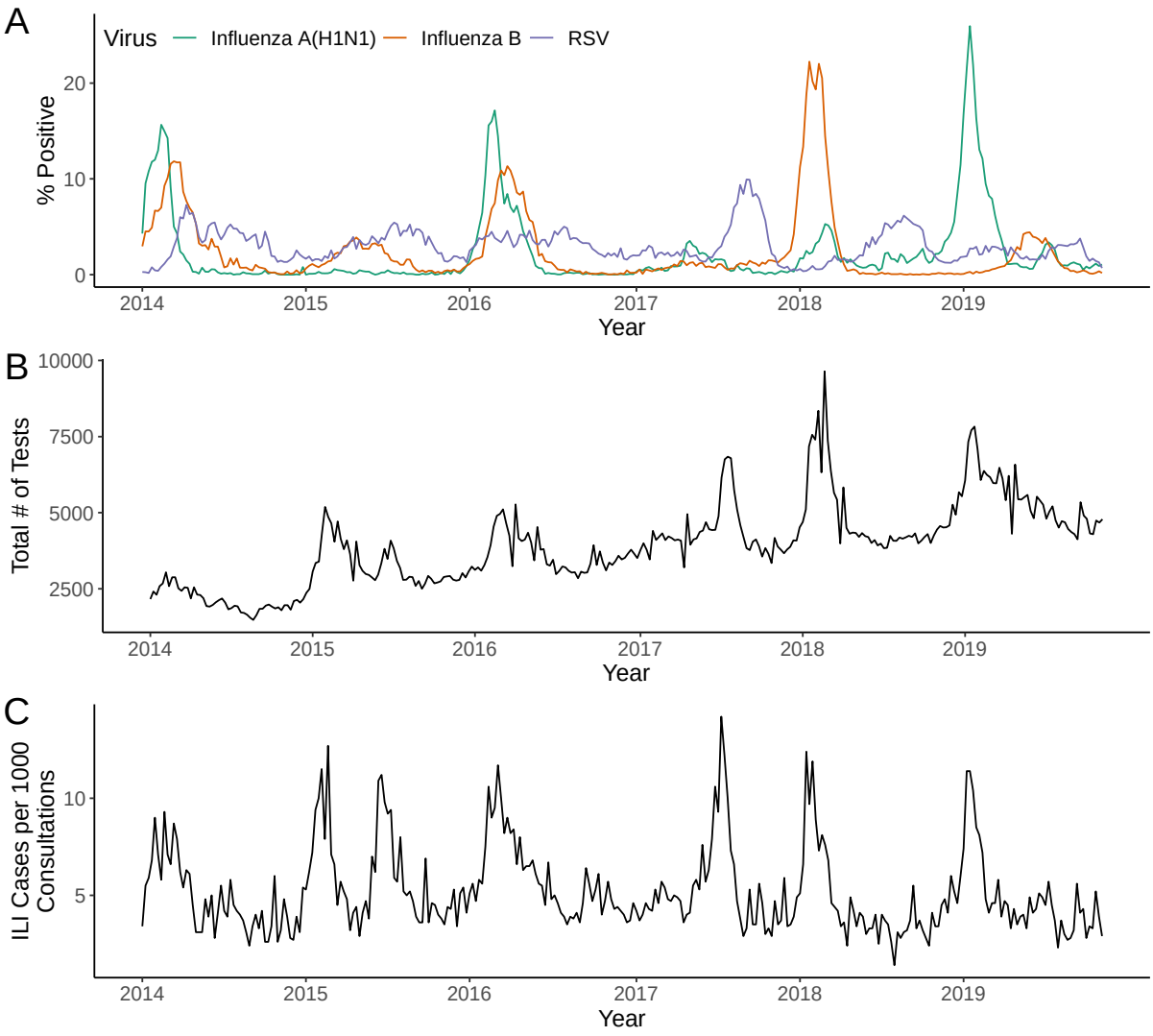

Figure 1. Respiratory virus positivity and ILI cases over the study period in Hong Kong. (A) Weekly percentage of tests positive for influenza A(H1N1), influenza B, and RSV; (B) weekly number of tests performed for respiratory viruses; (C) weekly number of cases of influenza-like illness reported by public out-patient clinics per 1000 consultations.

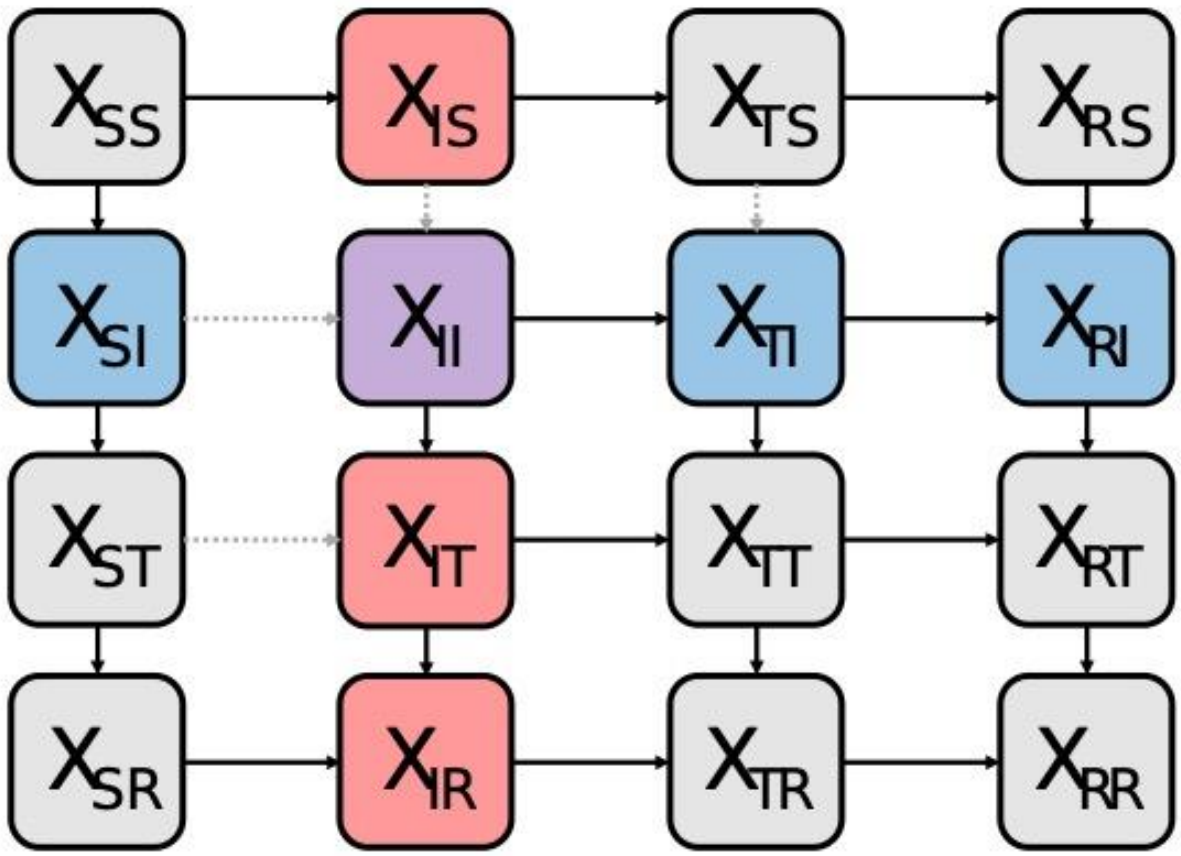

Figure 2. Schematic for the model of influenza and RSV cocirculation. Boxes represent the model states, where the first subscript indicates infection status with regard to influenza and the second subscript indicates infection status with regard to RSV (i.e., X_{IR} refers to those infected with influenza and recovered from RSV). Compartments containing individuals infected with influenza are shown in red, compartments with individuals infected with RSV are shown in blue, and the compartment containing coinfected individuals is shown in purple. Arrows represent possible transitions between compartments; the gray dotted arrows in particular indicate transitions that are influenced by the interaction effect.

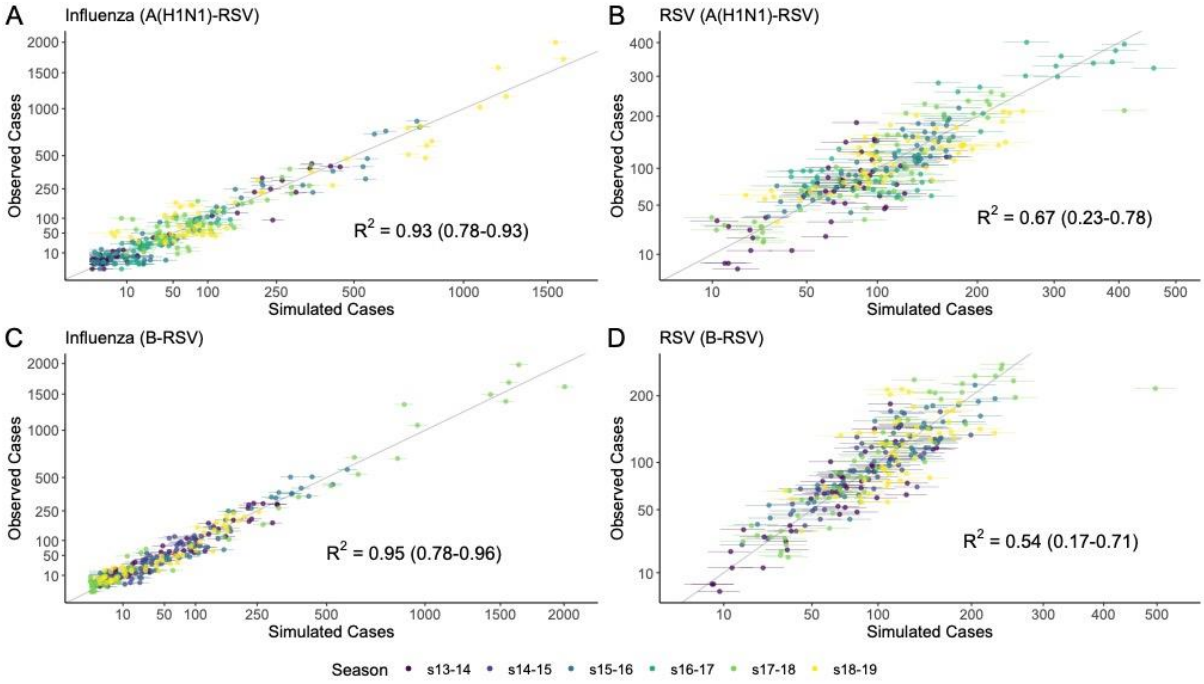

Figure 3. Cases simulated from the deterministic model at the MLE vs. observed case counts. More specifically, simulated case counts were taken to be the mean value of the observation model at each timepoint. Error bars represent the 95% prediction intervals, and colors indicate the season from which each point was taken. The gray line is the identity line, and represents perfect agreement between simulations and observations. Results are shown separately for influenza (A, C) and RSV (B, D), as well as for both the A(H1N1)-RSV virus-virus pair (A-B) and the B-RSV virus-virus pair (C-D). The R^2 values over all seasons combined, as well as the range of values by season, are shown. Note that both axes use a square root transformation.

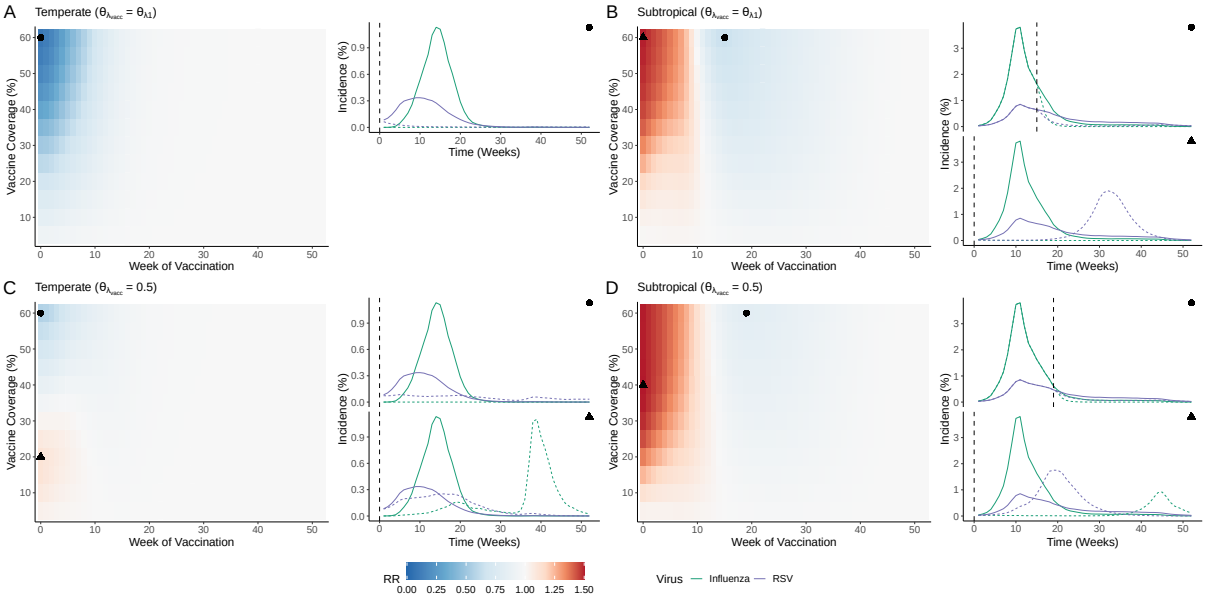

Figure 4. Impact of vaccination with LAIV on RSV attack rates. Heatmaps show the rate ratio of RSV attack rates in the presence of vaccination relative to the attack rates in the absence of vaccination (Equation 3) at a range of values for vaccine timing (x-axes) and coverage levels (y-axes). Values below 1.0 (indicating a decrease in attack rates) are shown in blue, and values above 1.0 (indicating an increase in attack rates) are shown in red. Lines indicate the simulated incidence of influenza (green) and RSV (purple) over the season in both the absence (solid lines) and presence (dotted lines) of vaccination. Points indicate the timing and coverage level of vaccination for each simulation; specifically, circles indicate the combination of vaccine timing and efficacy that yielded the greatest reduction in RSV attack rates, while triangles indicate the combination yielding the greatest increase. Results are shown for both temperate (A, C) and subtropical (B, D) scenarios. Results assuming a vaccine with the same influence on RSV susceptibility as natural influenza infection are shown in (A) and (B), while results assuming that vaccination reduces RSV susceptibility by half are shown in (C) and (D). For each scenario, a representative season was selected (2017-18 for the temperate scenario and 2018-19 for the subtropical scenario); results for all other seasons can be found in Supplementary Figure 10.

Declarations

Competing interests: MDdC received postdoctoral funding (2017–2019) from Pfizer and consulting fees from GSK. All other authors declare no competing interests.

Authors' Contributions: SCK conducted the analyses and wrote the first draft of the manuscript. JSC provided content expertise. MDdC conceived the study design and oversaw the analysis. All authors helped draft and approved the final version of, the manuscript.

Acknowledgments: We thank Laura Barrero Guevara for her helpful comments on the manuscript.

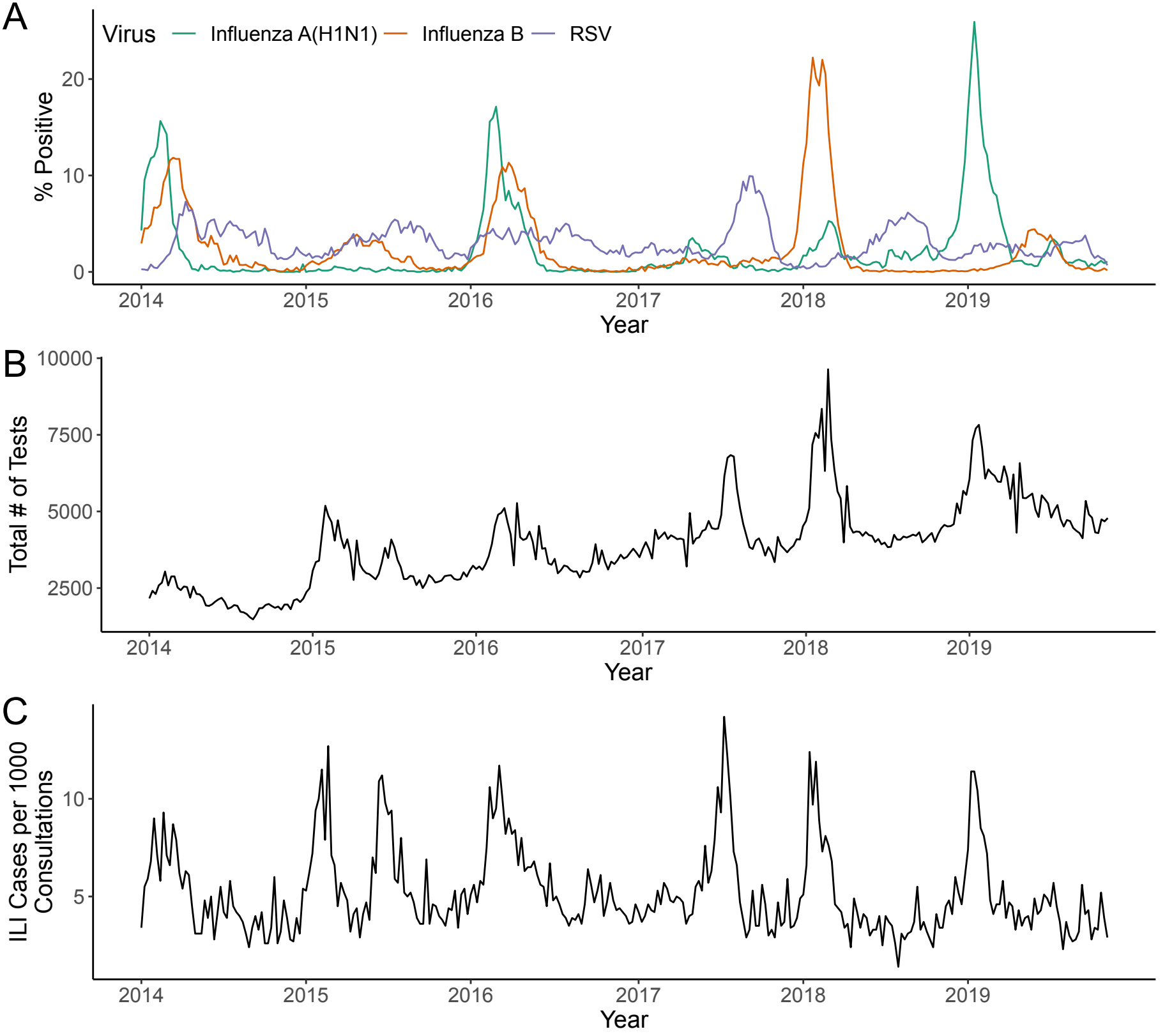
A
Virus
Influenza A(H1N1)
Influenza B
RSV
% Positive
0
10
20
2014
2015
2016
2017
2018
2019
Year
B
Total # of Tests
2500
5000
7500
10000
2014
2015
2016
2017
2018
2019
Year
C
ILI Cases per 1000 Consultations
5
10
2014
2015
2016
2017
2018
2019
Year

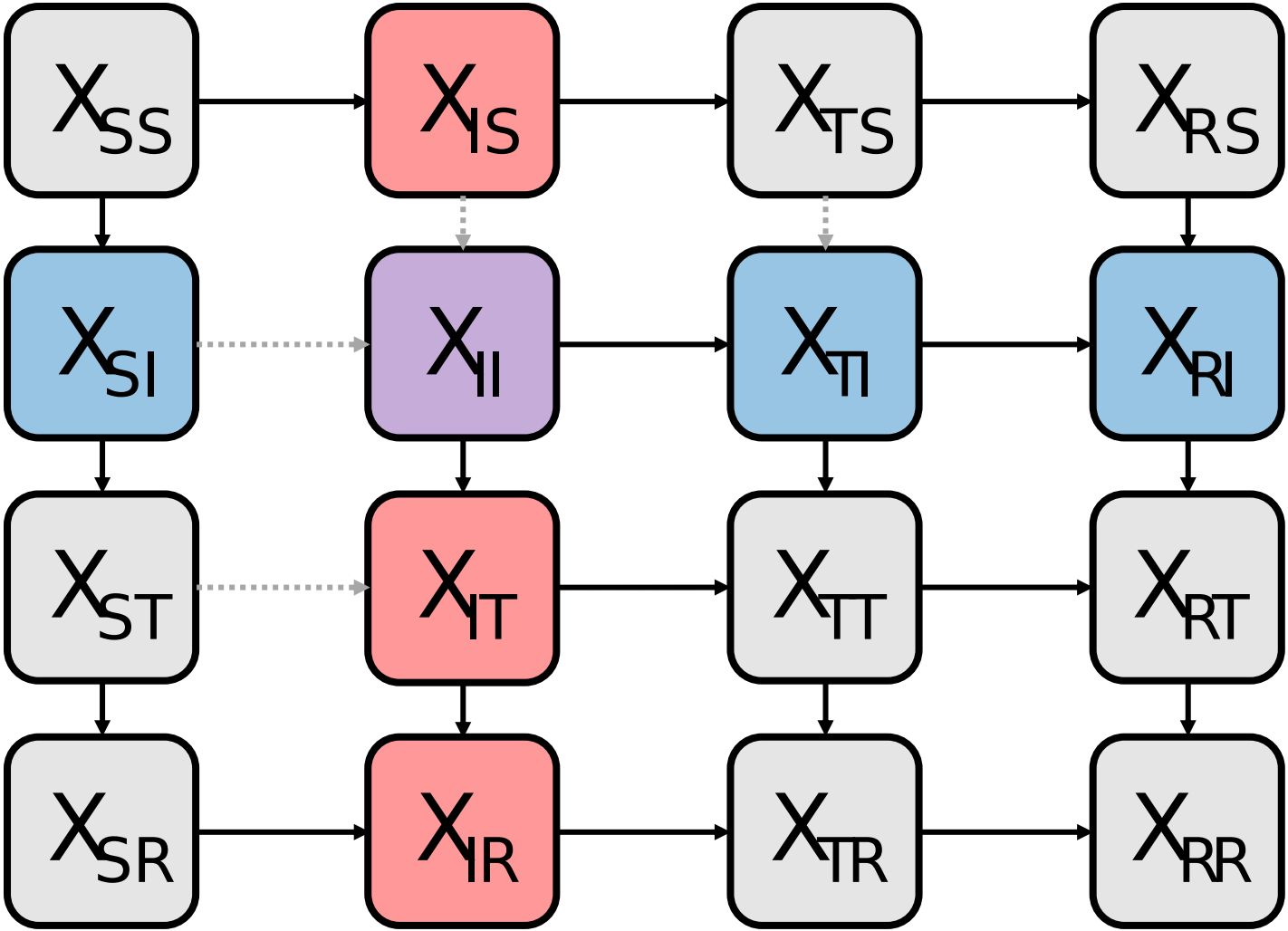
X_{SS}
X_{IS}
X_{TS}
X_{RS}
X_{SI}
X_{II}
X_{TI}
X_{RI}
X_{ST}
X_{IT}
X_{TT}
X_{RT}
X_{SR}
X_{IR}
X_{TR}
X_{RR}

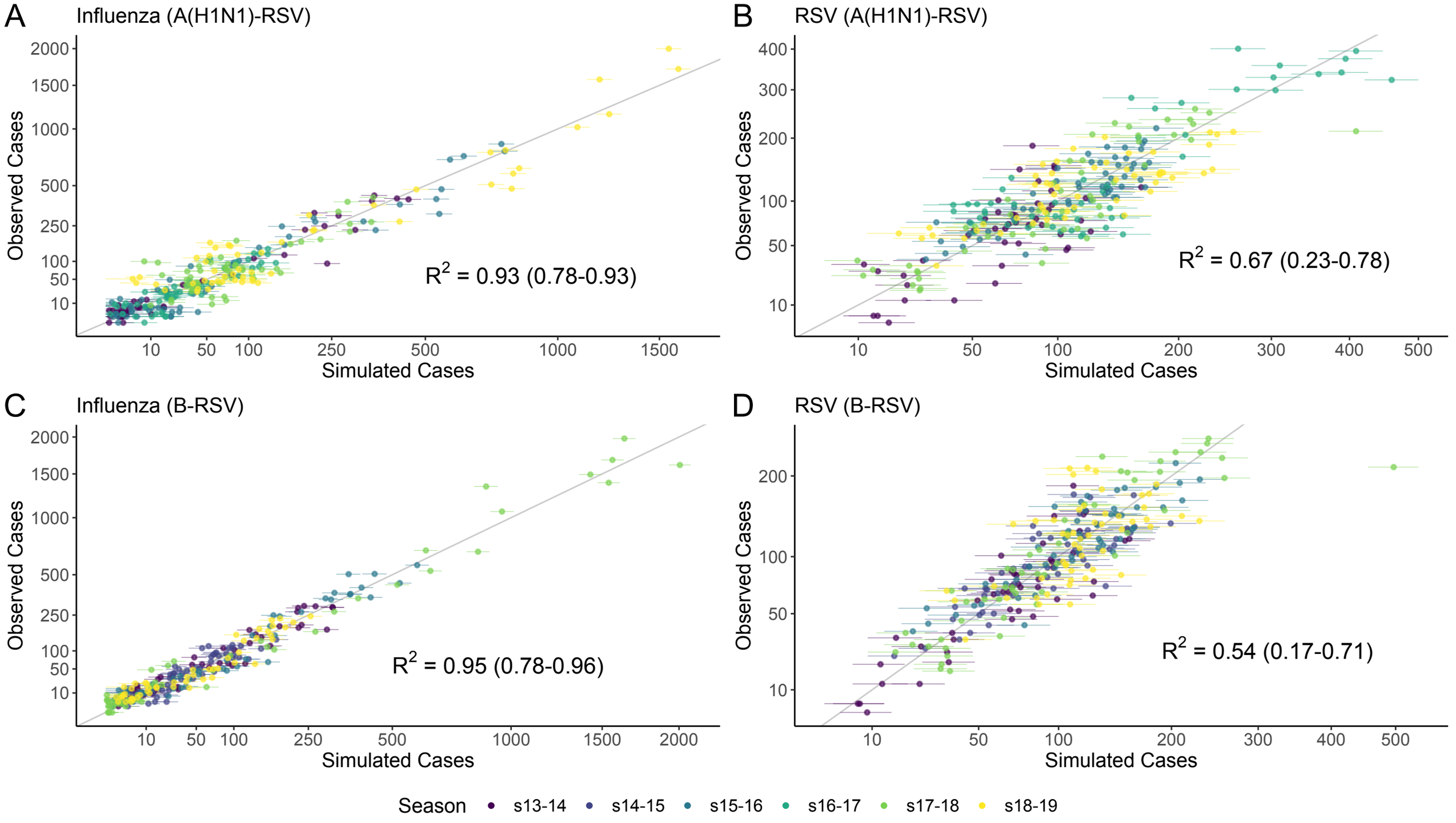
A
Influenza (A(H1N1)-RSV)
Observed Cases
Simulated Cases
R^2 = 0.93 (0.78-0.93)
B
RSV (A(H1N1)-RSV)
Observed Cases
Simulated Cases
R^2 = 0.67 (0.23-0.78)
C
Influenza (B-RSV)
Observed Cases
Simulated Cases
R^2 = 0.95 (0.78-0.96)
D
RSV (B-RSV)
Observed Cases
Simulated Cases
R^2 = 0.54 (0.17-0.71)
Season
s13-14
s14-15
s15-16
s16-17
s17-18
s18-19

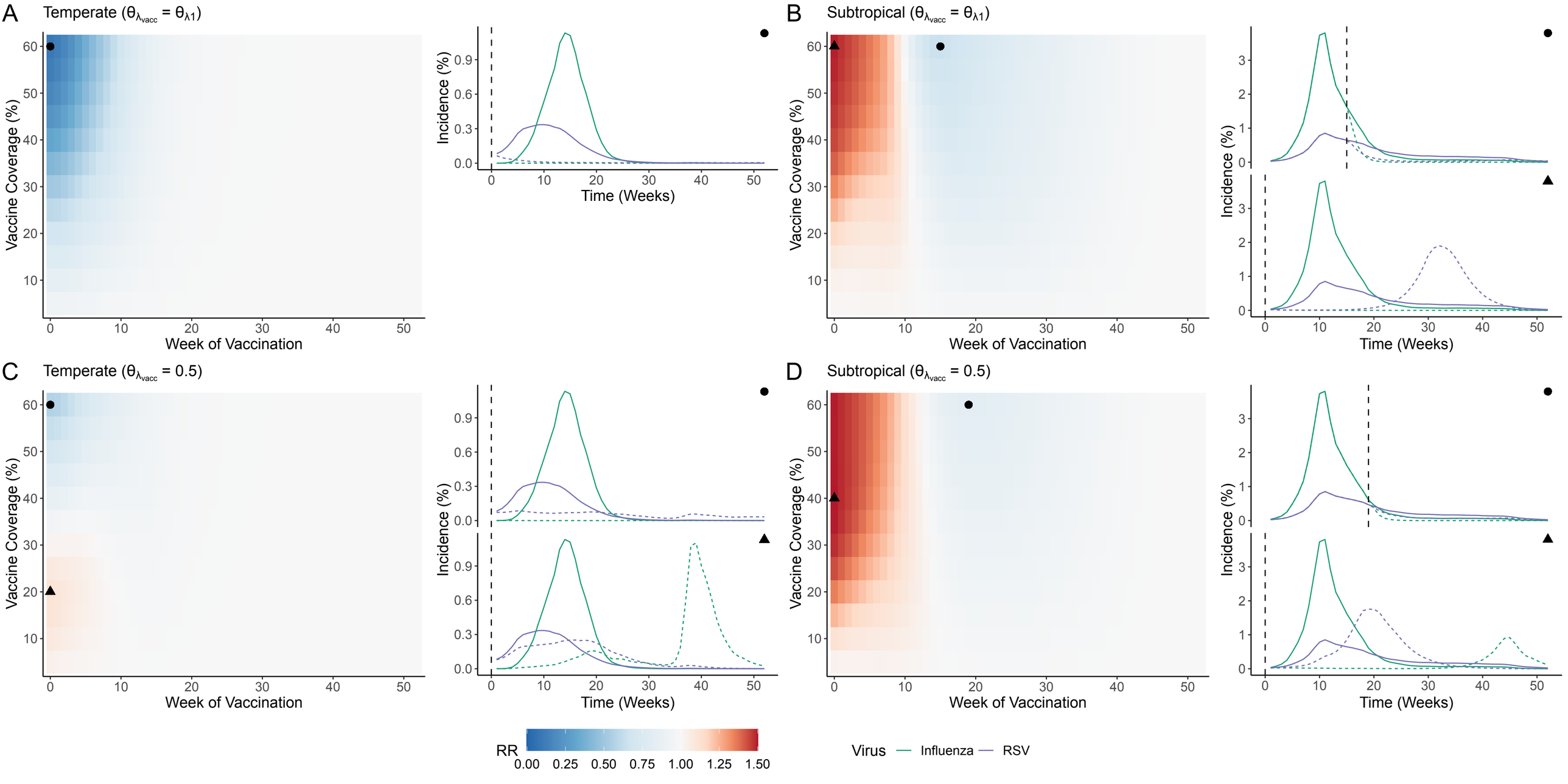
A
Temperate ($\theta_{\lambda_{vacc}} = \theta_{\lambda 1}$)
B
Subtropical ($\theta_{\lambda_{vacc}} = \theta_{\lambda 1}$)
C
Temperate ($\theta_{\lambda_{vacc}} = 0.5$)
D
Subtropical ($\theta_{\lambda_{vacc}} = 0.5$)
Vaccine Coverage (%)
Week of Vaccination
Incidence (%)
Time (Weeks)
RR
0.00 0.25 0.50 0.75 1.00 1.25 1.50
Virus
Influenza
RSV

Table 1. Descriptions and maximum likelihood estimates of all model parameters.

Parameter	Description	Fit Value (99% CI) H1 / RSV	Fit Value (99% CI) B / RSV	Season-Specific?
$\theta_{\lambda 1}$	Strength of the interaction effect of influenza on RSV	3.23×10^{-3} (0, 0.022)	3.14×10^{-5} (0, 0.118)	No
$\theta_{\lambda 2}$	Strength of the interaction effect of RSV on influenza	3.46×10^{-15} (0, 0.111)	0.531 (0.232, 1.0)	No
δ_1	Rate of loss of cross-protection against RSV after influenza infection	0.063 (0.055, 0.073)	0.079 (0.056, 0.107)	No
d_2	Rate of loss of cross-protection against influenza after RSV infection, relative to δ_1	2.15 (1.47, 2.86)	2.4×10^{8} (0.03, ∞)	No
ρ_1	Composite reporting rate/scaling parameter for influenza	0.078 (0.070, 0.084)	0.083 (0.071, 0.085)	No
ρ_2	Composite reporting rate/scaling parameter for RSV	0.056 (0.047, 0.063)	0.060 (0.048, 0.067)	No
η_{temp1}	Impact of temperature on influenza	-0.29 (-0.30, -0.26)	0.041 (0.023, 0.048)	No
η_{AH1}	Impact of absolute humidity on influenza	0.44 (0.42, 0.46)	0.007 (-0.001, 0.039)	No
η_{temp2}	Impact of temperature on RSV	-0.40 (-0.43, -0.34)	-0.20 (-0.22, -0.13)	No
η_{AH2}	Impact of absolute humidity on RSV	0.46 (0.41, 0.50)	0.21 (0.16, 0.26)	No
α	Amplitude of seasonality in reporting and background consultation rates	0.62 (0.57, 0.68)	0.75 (0.71, 0.77)	No
φ	Time of maximum ρ_1/ρ_2	46.3 (45.9, 47.0)	51.2 (51.0, 51.9)	No
Ri1	Initial effective reproductive number for influenza	See Supplementary Figure 3		Yes
Ri2	Initial effective reproductive number for RSV	See Supplementary Figure 3		Yes
I10	Initial proportion of the population infected with influenza	See Supplementary Figure 3		Yes
I20	Initial proportion of the population infected with RSV	See Supplementary Figure 3		Yes
R10	Initial proportion of the population immune to influenza only	See Supplementary Figure 3		Yes
R20	Initial proportion of the population immune to RSV only	See Supplementary Figure 3		Yes
R120	Initial proportion of the population immune to both influenza and RSV	See Supplementary Figure 3		Yes